

A branched-chain amino acid metabolite drives vascular fatty acid transport and causes insulin resistance

Cholsoon Jang^{1,2,8}, Sungwhan F Oh^{3,8}, Shogo Wada¹, Glenn C Rowe^{2,7}, Laura Liu², Mun Chun Chan², James Rhee^{2,4}, Atsushi Hoshino¹, Boa Kim¹, Ayon Ibrahim¹, Luisa G Baca², Esl Kim², Chandra C Ghosh², Samir M Parikh², Aihua Jiang², Qingwei Chu¹, Daniel E Forman⁵, Stewart H Lecker², Saikumari Krishnaiah¹, Joshua D Rabinowitz⁶, Aalim M Weljie¹, Joseph A Baur¹, Dennis L Kasper³ & Zoltan Arany¹

Epidemiological and experimental data implicate branched-chain amino acids (BCAAs) in the development of insulin resistance, but the mechanisms that underlie this link remain unclear^{1–3}. Insulin resistance in skeletal muscle stems from the excess accumulation of lipid species⁴, a process that requires blood-borne lipids to initially traverse the blood vessel wall. How this trans-endothelial transport occurs and how it is regulated are not well understood. Here we leveraged PPARGC1a (also known as PGC-1 α ; encoded by *Ppargc1a*), a transcriptional coactivator that regulates broad programs of fatty acid consumption, to identify 3-hydroxyisobutyrate (3-HIB), a catabolic intermediate of the BCAA valine, as a new paracrine regulator of trans-endothelial fatty acid transport. We found that 3-HIB is secreted from muscle cells, activates endothelial fatty acid transport, stimulates muscle fatty acid uptake *in vivo* and promotes lipid accumulation in muscle, leading to insulin resistance in mice. Conversely, inhibiting the synthesis of 3-HIB in muscle cells blocks the ability of PGC-1 α to promote endothelial fatty acid uptake. 3-HIB levels are elevated in muscle from *db/db* mice with diabetes and from human subjects with diabetes, as compared to those without diabetes. These data unveil a mechanism in which the metabolite 3-HIB, by regulating the trans-endothelial flux of fatty acids, links the regulation of fatty acid flux to BCAA catabolism, providing a mechanistic explanation for how increased BCAA catabolic flux can cause diabetes.

PGC-1 α in skeletal muscle induces broad genetic programs, including mitochondrial biogenesis and fatty acid β -oxidation^{5,6}. PGC-1 α also induces the paracrine activation of angiogenesis, thereby coordinating the consumption of fatty acids in mitochondria with their delivery via blood vessels⁷. We reasoned that to maximize the delivery of fatty acids to muscle, PGC-1 α might also instruct blood vessels to increase

trans-endothelial fatty acid transport from the vessel lumen to the extraluminal myofibers, a process that remains poorly understood.

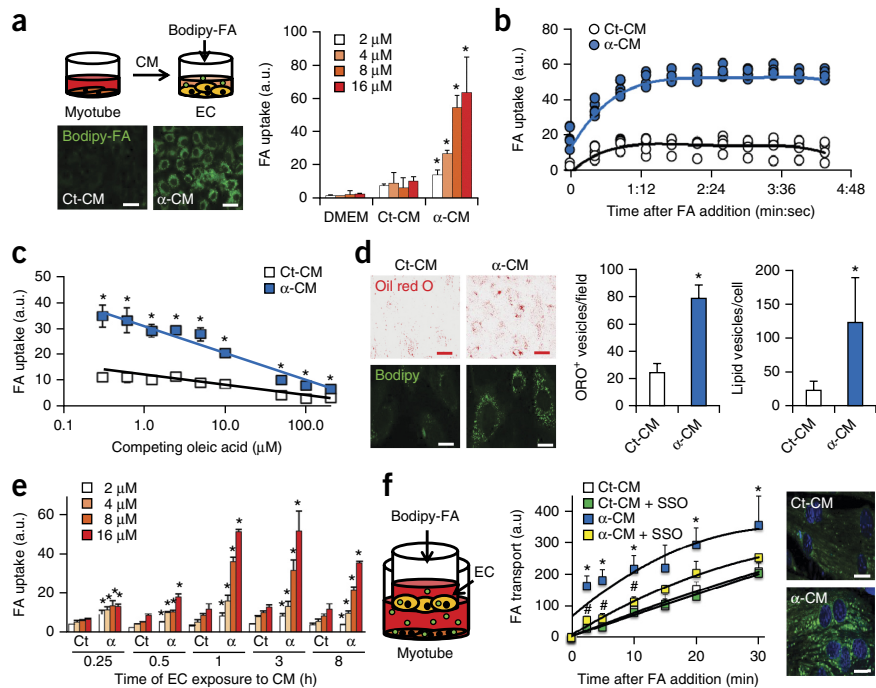
To test this hypothesis, we devised an assay in which conditioned medium from skeletal myotubes, derived from an immortal line of mouse myoblasts (C2C12 cells), was added to human umbilical vein endothelial cells (HUVECs), after which we used the fluorescent fatty acid analog Bodipy-C12 to measure the ability of the HUVECs to take up fatty acids (Supplementary Fig. 1a). Notably, conditioned medium from myotubes that overexpressed human PGC-1 α (α -CM), using infection with either adenovirus (Fig. 1a) or, in multiple cell lines, retrovirus (Supplementary Fig. 1b–d), dramatically increased the amount of fatty acid uptake in HUVECs when compared to control conditioned medium (Ct-CM) from myotubes expressing GFP. This result suggests that a PGC-1 α -regulated paracrine factor induces endothelial fatty acid uptake. The uptake of fatty acid was rapid (Fig. 1b); saturated by high fatty acid concentrations (Supplementary Fig. 2a); competed with by equimolar unlabeled oleic acid (Fig. 1c); limited to the uptake of long-chain fatty acids (Supplementary Fig. 2b); and persistent after dilution of α -CM (Supplementary Fig. 2c). Taken together, these observations strongly suggest that the uptake of fatty acid is a specific, and probably protein-mediated, process. The prolonged exposure of endothelial cells to α -CM increased intracellular lipid levels as compared to cells exposed to Ct-CM, as measured by staining with oil red O or unconjugated Bodipy (Fig. 1d). The stimulation of fatty acid uptake by α -CM was specific to endothelial cells: only one of ten non-endothelial cell types showed increased uptake of Bodipy-C12 after incubation with α -CM, whereas every endothelial cell type tested did (Supplementary Fig. 2d). The induction of fatty acid uptake by endothelial cells occurred within 15–60 min of exposure to α -CM (Fig. 1e) and was adenosine triphosphate (ATP) dependent (Supplementary Fig. 2e). α -CM strongly induced fatty acid flux across a tight endothelial monolayer, and this flux was blocked by sulfo-*N*-succinimidyl oleate (SSO), an inhibitor of fatty

¹Perelman School of Medicine, University of Pennsylvania, Philadelphia, Pennsylvania, USA. ²Beth Israel Deaconess Medical Center, Harvard Medical School, Boston, Massachusetts, USA. ³Department of Microbiology and Immunobiology, Harvard Medical School, Boston, Massachusetts, USA. ⁴Department of Anesthesia, Critical Care, and Pain Medicine, Massachusetts General Hospital, Boston, Massachusetts, USA. ⁵Department of Medicine, University of Pittsburgh, Pittsburgh, Pennsylvania, USA. ⁶Lewis-Sigler Institute for Integrative Genomics, Princeton University, Princeton, New Jersey, USA. ⁷Present address: Department of Medicine, University of Alabama at Birmingham, Birmingham, Alabama, USA. ⁸These authors contributed equally to this work. Correspondence should be addressed to Z.A. (zarany@mail.med.upenn.edu).

Received 11 December 2015; accepted 5 February 2016; published online 7 March 2016; doi:10.1038/nm.4057

Figure 1 PGC-1 α expression in muscle cells induces the secretion of a paracrine activity that stimulates endothelial fatty acid (FA) transport.

(a) Experimental strategy (top), representative images (bottom) and quantification (right) of Bodipy-FA (2–16 μ M) uptake by endothelial cells (ECs) after exposure to control Dulbecco's modified Eagle's medium (DMEM) culture, conditioned media (CM) from control myotubes expressing GFP (Ct-CM) or myotubes expressing PGC-1 α (α -CM). a.u., arbitrary units. Scale bars, 50 μ m. (b,c) Bodipy-FA (8 μ M) uptake by HUVECs treated with Ct-CM or α -CM at different time points (b), or in the presence of the indicated concentrations of unlabeled oleic acid for 5 min (c). (d) Staining by oil red O (ORO) of intracellular neutral lipids in HUVECs after prolonged exposure (24 h) to α -CM. Representative images (left) and quantification of ORO-positive lipid vesicles (middle) and Bodipy-positive lipid vesicles (right) are shown. Red scale bars, 50 μ m; white scale bars, 10 μ m. (e) Uptake of the indicated concentrations of Bodipy-FA by HUVECs after incubation with either Ct-CM (Ct) or α -CM (α) for the indicated durations. (f) Experimental strategy (left). Quantification of Bodipy-FA (8 μ M) transport across a tight endothelial cell monolayer treated with either Ct-CM or α -CM, with or without the fatty acid transport inhibitor SSO (middle). Representative images of myotubes that have taken up Bodipy-FA (green) transported through the monolayer (right). Scale bars, 10 μ m. Student's *t* test; **P* < 0.05 versus control; #*P* < 0.05 versus α -CM for all panels. Two-way analysis of variance (ANOVA) was used for f. Data are mean \pm s.d. (s.d.) of at least three biological replicates.



acid transport (Fig. 1f and Supplementary Fig. 2f–h). Conversely, an endothelial monolayer treated with conditioned medium from myotubes that lacked both PGC-1 α and PGC-1 β —a related PGC-1 family member, encoded by *Ppargc1b*—showed reduced amounts of fatty acid transport as compared to endothelial cells treated with CM from wild-type myotubes (Supplementary Fig. 2i–k). Taken together, these data demonstrate the existence of one or more paracrine factors, induced in myotubes by PGC-1 α , that stimulate endothelial fatty acid uptake and transport.

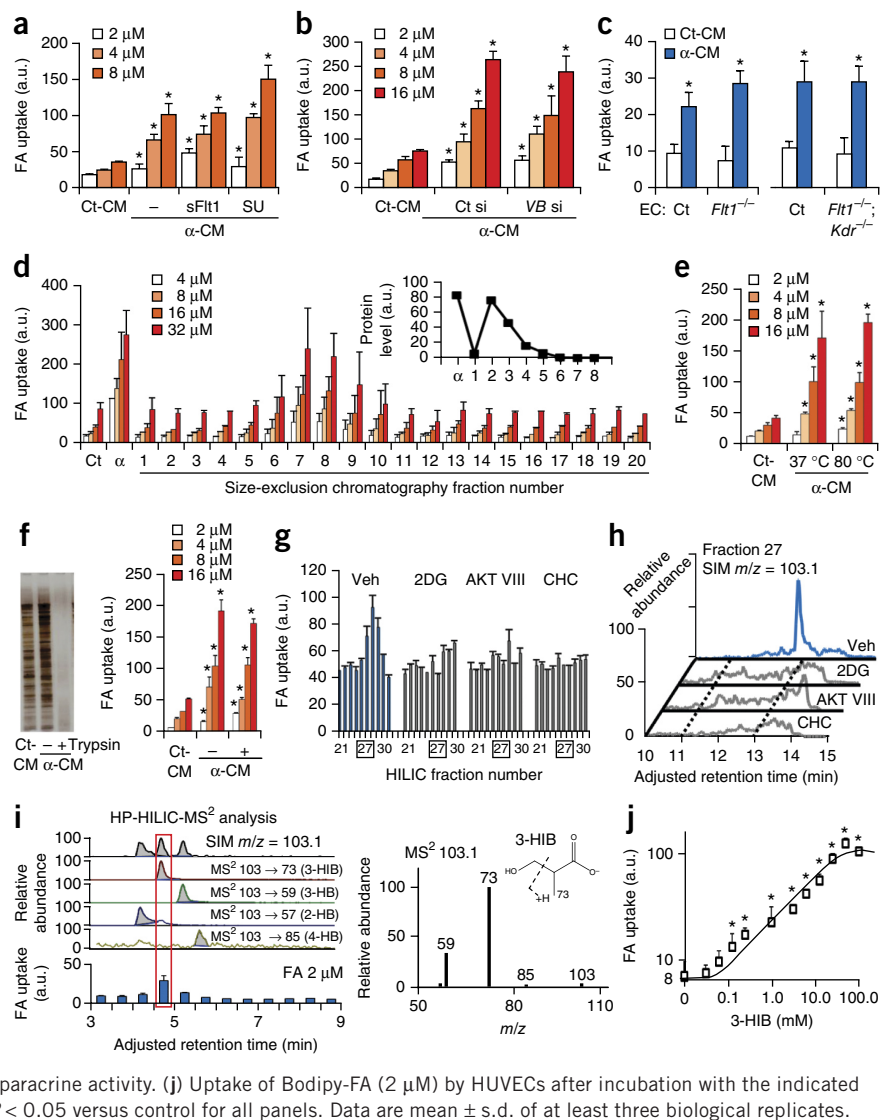
Vascular endothelial growth factor B (VEGF-B, encoded by *Vegfb*) has recently been shown to promote the amount of endothelial fatty acid taken up via its cognate receptor fms-related tyrosine kinase 1, FLT1 (also known as VEGFR1, encoded by *Flt1*)⁸, raising the possibility that VEGF-B might be the relevant paracrine factor in α -CM. Consistent with this notion, PGC-1 α induced the expression of VEGF-B in mice (Supplementary Fig. 3a). However, the neutralization of VEGF-B using a neutralizing soluble, splice variant-encoded form of FLT1 (sFLT1) or by receptor inhibition using a VEGFR tyrosine kinase inhibitor (SU11248) failed to block the activity of α -CM, despite efficient inhibition of VEGF-B signaling (Fig. 2a and Supplementary Fig. 3b,c). Knockdown of *Vegfb* in myotubes (Fig. 2b and Supplementary Fig. 3d) or genetic deletion of either or both of *Flt1* and *Kdr* (also known as *Flk1* or *Vegfr2*, encoding the kinase insert domain protein receptor) in endothelial cells also failed to inhibit α -CM activity (Fig. 2c and Supplementary Fig. 3e–g). The paracrine factor in α -CM is thus not VEGF-B.

To identify the paracrine factor in α -CM, we fractionated α -CM using size-exclusion chromatography. The fatty acid uptake-inducing activity was found in fractions containing small molecules, but few proteins (Fig. 2d and Supplementary Fig. 3h). Treatment of α -CM at 80 °C (Fig. 2e), with trypsinization (Fig. 2f) or with charcoal (Supplementary Fig. 3i), failed to abolish the activity, suggesting that

the paracrine factor is a hydrophilic nonprotein metabolite(s). Initial efforts to identify differences between α -CM and control conditioned medium using mass spectrometry revealed thousands of peaks—too many to identify individually. We next searched for compounds that could block the production of fatty acid uptake-inducing activity from PGC-1 α -expressing C2C12 myotubes. We identified a number of such compounds, including inhibitors of the phosphoinositide-3-kinase (PI3K) pathway (compounds targeting PI3K, AKT1 or mTOR complex 2), as well as inhibitors of glycolysis (2-deoxy-glucose (2DG)) and of monocarboxylate transport (2-cyano-3-(4-hydroxyphenyl)-2-propenoic acid, CHC) (Supplementary Fig. 4a–c). None of these inhibitors directly affected fatty acid uptake by endothelial cells (Supplementary Fig. 4d), a result that is consistent with the concept that these compounds act on muscle cells to block the production and/or secretion of the paracrine factor. Pyruvate supplementation partially restored the inhibitory effects of the AKT1 inhibitor and of 2DG, but not of CHC (Supplementary Fig. 4e).

The identification of these inhibitors allowed for further purification of the paracrine factor(s), by using discerning negative controls that minimized differences between conditioned media (Supplementary Fig. 4f). The conditioned media were first treated with charcoal to remove hydrophobic compounds. They were then fractionated via open-column silica-gel chromatography (Supplementary Fig. 5a). The active fractions from this fractionation still contained too many mass spectrophotometric peaks for us to identify the active factor; the fractions were therefore further subjected to orthogonal fractionation by high-pressure hydrophilic-interaction liquid chromatography (HP-HILIC) (Supplementary Fig. 5b). Evaluation of active fractions by mass spectrometry revealed a peak with a molecular weight of 104.1 (M-H = 103.1); this peak was absent in parallel, inactive fractions from control media of cells pre-treated with 2DG, AKT1 inhibitor (AKT VIII), or CHC (Fig. 2g,h). Among multiple compounds that

Figure 2 Identification of 3-HIB as the paracrine factor. (a) Uptake of the indicated concentrations of Bodipy-FA by HUVECs after incubation with conditioned media from myotubes expressing GFP (Ct-CM) or PGC-1 α (α -CM), after treatment of the endothelial cells with sFlt1 or SU11248 (SU). (b) Uptake of the indicated concentrations of Bodipy-FA by HUVECs after incubation with Ct-CM or with CM from PGC-1 α -expressing myotubes treated with control siRNA (Ct si) or *Vegfb* siRNA (VB si). (c) Uptake of Bodipy-FA (2 μ M) by endothelial cells (EC) isolated from *Flt1*^{fllox/fllox} or *Flt1*^{fllox/fllox}; *Kdr*^{fllox/fllox} mice, followed by infection with adenovirus expressing GFP (Ct) or Cre recombinase (*Flt1*^{-/-} or *Flt1*^{-/-}; *Kdr*^{-/-}), and subsequent incubation with Ct-CM or α -CM. (d–f) Uptake of the indicated concentrations of Bodipy-FA by HUVECs after incubation with size-exclusion chromatography fractions of α -CM (d), α -CM that had been heat-inactivated at the indicated temperature (e) or α -CM treated with trypsin (f). Ct-CM and α -CM were used as negative and positive controls, respectively. In d, protein levels of the fractions are shown in the inset. Silver staining of Ct-CM, α -CM and α -CM treated with trypsin is shown in f (left). (g) Uptake of Bodipy-FA (8 μ M) by HUVECs after incubation with HILIC fractions of conditioned medium from PGC-1 α -expressing myotubes that had been treated with vehicle (Veh) or the indicated inhibitors. (h) Selective ion monitoring (SIM) of *m/z* = 103.1 in HILIC fraction 27 of conditioned medium from PGC-1 α -expressing myotubes that had been treated with vehicle (Veh) or the indicated inhibitors. (i) SIM of *m/z* = 103.1 in HP-HILIC fractions (top left) and tandem-mass spectrometry (MS²) analysis (right) and uptake of Bodipy-FA by HUVECs after incubation with HP-HILIC fractions (bottom left). Red box (left) highlights the paracrine activity. (j) Uptake of Bodipy-FA (2 μ M) by HUVECs after incubation with the indicated concentrations of 3-HIB for 1 h. Student's *t* test; **P* < 0.05 versus control for all panels. Data are mean \pm s.d. of at least three biological replicates.



were candidates for the active factor, as determined by the retention time of the unknown compound in the HILIC column, four isobaric hydroxybutyrates potentially corresponded to its molecular weight (Supplementary Fig. 5c). Bioactivity was correlated with a molecule with a tandem mass fingerprint of 103 \rightarrow 73, which, of the four identified candidates, was consistent with 3-HIB (Fig. 2i). Further matching of the chromatographic properties and tandem mass spectra of the active factor to synthetic standards unambiguously confirmed this conclusion. The addition of synthetic 3-HIB to the culture medium, as compared to the addition of vehicle only, was sufficient to increase Bodipy-fatty acid (Bodipy-FA) uptake by HUVECs (Fig. 2j); Bodipy-FA transport across a tight monolayer of endothelial cells (Supplementary Fig. 6a–c); and the transport of ¹³C-labeled palmitate across a tight monolayer of endothelial cells. This transport was followed by uptake and incorporation of the labeled palmitate into the tricarboxylic acid (TCA) cycle intermediates of the myotubes on the other side of the monolayer (Supplementary Fig. 6d). These data thus unequivocally identify 3-HIB as the active component in the fractions.

3-HIB is an intermediate of valine catabolism. It is derived from 3-hydroxyisobutyryl-coenzyme A (HIBC) by HIBChydrolase (HIBCH,

encoded by *Hibch*), and it is subsequently catabolized by 3-HIB dehydrogenase (HIBADH, encoded by *Hibadh*), leading to the formation of propionyl-CoA (Fig. 3a). ¹³C-labeling of valine in PGC-1 α -expressing myotubes led to nearly complete ¹³C labeling of 3-HIB (Fig. 3b and Supplementary Fig. 6e,f). Moreover, the fatty acid uptake-inducing activity of α -CM required the presence of valine in the culture media of the myotubes (Supplementary Fig. 6g), demonstrating that 3-HIB in α -CM is indeed derived from valine. PGC-1 α overexpression in myotubes induced the expression of nearly every enzyme of BCAA catabolism (Fig. 3c and Supplementary Fig. 7a,b)⁹. This result is consistent with the notion that the increased levels of 3-HIB in α -CM (Supplementary Fig. 7c) reflect PGC-1 α -induced catabolism of valine. PGC-1 β overexpression also induced expression of the same genes that were induced by PGC-1 α , whereas the deletion of both PGC-1 α and PGC-1 β resulted in repression of valine catabolic genes (Supplementary Fig. 7d–f). Knockdown of *Hibch* in myotubes (Supplementary Fig. 7g) nearly abolished the α -CM-induced uptake of fatty acids by endothelial cells (Fig. 3d). Conversely, knockdown of *Hibadh* (encoding the downstream enzyme) in myotubes enhanced the effect of α -CM on fatty acid uptake (Fig. 3d). Similarly, knockdown of *Hibadh* in mouse skeletal muscle *in vivo*

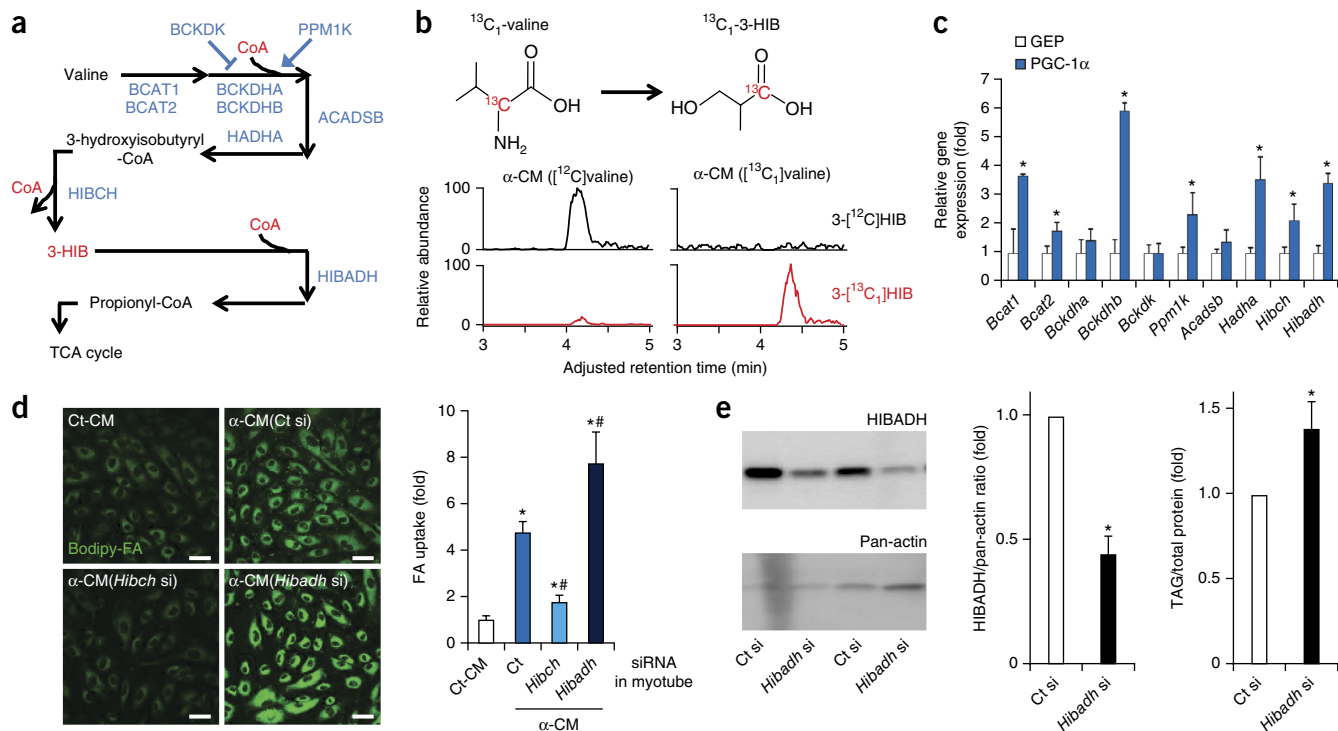


Figure 3 3-HIB is generated from valine catabolism that is induced by PGC-1 α , and it stimulates endothelial fatty acid uptake. **(a)** Schematic of the valine catabolism pathway. BCAT, branched-chain aminotransferase; BCKDH, branched-chain α -keto acid dehydrogenase; BCKDK, branched-chain ketoacid dehydrogenase kinase; PPM1K, protein phosphatase $\text{Mg}^{2+}/\text{Mn}^{2+}$ -dependent 1K; ACADSB, short/branched chain acyl-CoA dehydrogenase; HADHA, hydroxyacyl-CoA dehydrogenase alpha subunit. **(b)** Chemical structures of ^{13}C -labeled valine (top left) and ^{13}C -labeled 3-HIB derived from ^{13}C -labeled valine (top right). The relative abundance of ^{12}C -3-HIB and ^{13}C -labeled 3-HIB in conditioned medium from PGC-1 α -expressing myotubes incubated with ^{12}C -valine (bottom left) and ^{13}C -labeled valine (bottom right). **(c)** qPCR analysis of valine metabolic gene expression in myotubes expressing either PGC-1 α or a GFP control. **(d)** Representative images of HUVECs that have taken up Bodipy-FA (left) and quantification (right) after exposure of the cells to conditioned medium from GFP-expressing myotubes (Ct si) or from PGC-1 α -expressing myotubes (α -CM) that had been treated with *Hibch* siRNA or *Hibadh* siRNA. Scale bars, 50 μm . **(e)** Immunoblot for HIBADH in mouse skeletal muscle after injection of intact animals with control (Ct si) or *Hibadh* (*Hibadh* si) siRNA (left); quantification of HIBADH abundance (middle); and muscle triacylglyceride (TAG) levels (right). $n = 8$ per group. Student's t test; * $P < 0.05$ versus control; # $P < 0.05$ versus α -CM for all panels. Two-way ANOVA for **d**. Data are mean \pm s.d. of at least three biological replicates.

increased triglyceride levels in the muscle when compared to those in control siRNA-injected mouse muscle (**Fig. 3e**). Endothelial cells (HUVECs) express the valine catabolic enzymes at much lower levels than does human skeletal muscle (**Supplementary Fig. 7h**), and knockdown of *HIBADH* in HUVECs did not affect fatty acid uptake (**Supplementary Fig. 7i,j**). Taken together, these data demonstrate that PGC-1 α in myotubes induces the catabolism of valine to 3-HIB, which then acts as a paracrine factor to stimulate endothelial fatty acid uptake.

Fatty acid transport protein (FATP) 3 (encoded by *FATP3*) and FATP4 (encoded by *FATP4*), as well as CD36, have been proposed to act as transporters of fatty acids in endothelial cells⁸. Knockdown of *FATP3* or *FATP4* in HUVECs led to decreased fatty acid uptake in response to α -CM or 3-HIB treatment, as compared to control-siRNA transfected HUVECs, and primary endothelial cells isolated from *Fatp4* knockout (KO) mice had decreased fatty acid uptake as compared to WT cells (**Supplementary Fig. 8a–c**). CD36 deficiency, in either HUVECs with *CD36* knockdown or primary endothelial cells isolated from *Cd36* KO mice, had less of an effect on fatty acid uptake than did *FATP3* or *FATP4* deficiency (**Supplementary Fig. 8d–g**). The uptake of fatty acid by endothelial cells in response to 3-HIB is thus largely mediated by *FATP3* and *FATP4*. Notably, neither *Fatp3* or *Fatp4* mRNA or protein levels were affected by either α -CM or 3-HIB treatment (**Supplementary Fig. 8h–k**), suggesting that post-translational

mechanisms are probably involved. This notion is consistent with the rapid response of endothelial cells to α -CM (**Fig. 1e**).

The majority of the genes that mediate valine catabolism were induced in the muscle of mice that transgenically overexpress PGC-1 α or PGC-1 β under control of the muscle-specific muscle creatine kinase promoter (MCK- α and MCK- β mice, respectively^{10,11}) (**Fig. 4a** and **Supplementary Fig. 9a**). Conversely, the expression of these genes was repressed in mice that lack both PGC-1 α and PGC-1 β in their skeletal muscle (**Supplementary Fig. 9b**). 3-HIB levels were increased in the skeletal muscle of MCK- α mice compared to littermate controls (**Fig. 4b**), consistent with an increase in the catabolism of valine, whereas BCAA levels are reduced¹². Fatty acid uptake in the skeletal muscle of MCK- α mice was dramatically increased *in vivo* (**Fig. 4c**), as shown noninvasively with the use of a luciferin-fatty acid conjugate; fatty acids linked to luciferin are released upon entry of the conjugate into cells, enabling the quantification of fatty acid uptake *in vivo* via luminometry in luciferase-expressing mice¹³. These findings are consistent with the seemingly paradoxical observation that MCK- α mice accumulate excess lipid in their muscle, leading to lipotoxicity and insulin resistance¹⁴. Similar glucose intolerance was observed in MCK- β mice (**Supplementary Fig. 9c**); conversely, glucose tolerance was improved and lipid levels were decreased in mice lacking both PGC-1 α and PGC-1 β in their skeletal muscle (**Supplementary Fig. 9d,e**). Altered 3-HIB secretion thus probably contributes to altered

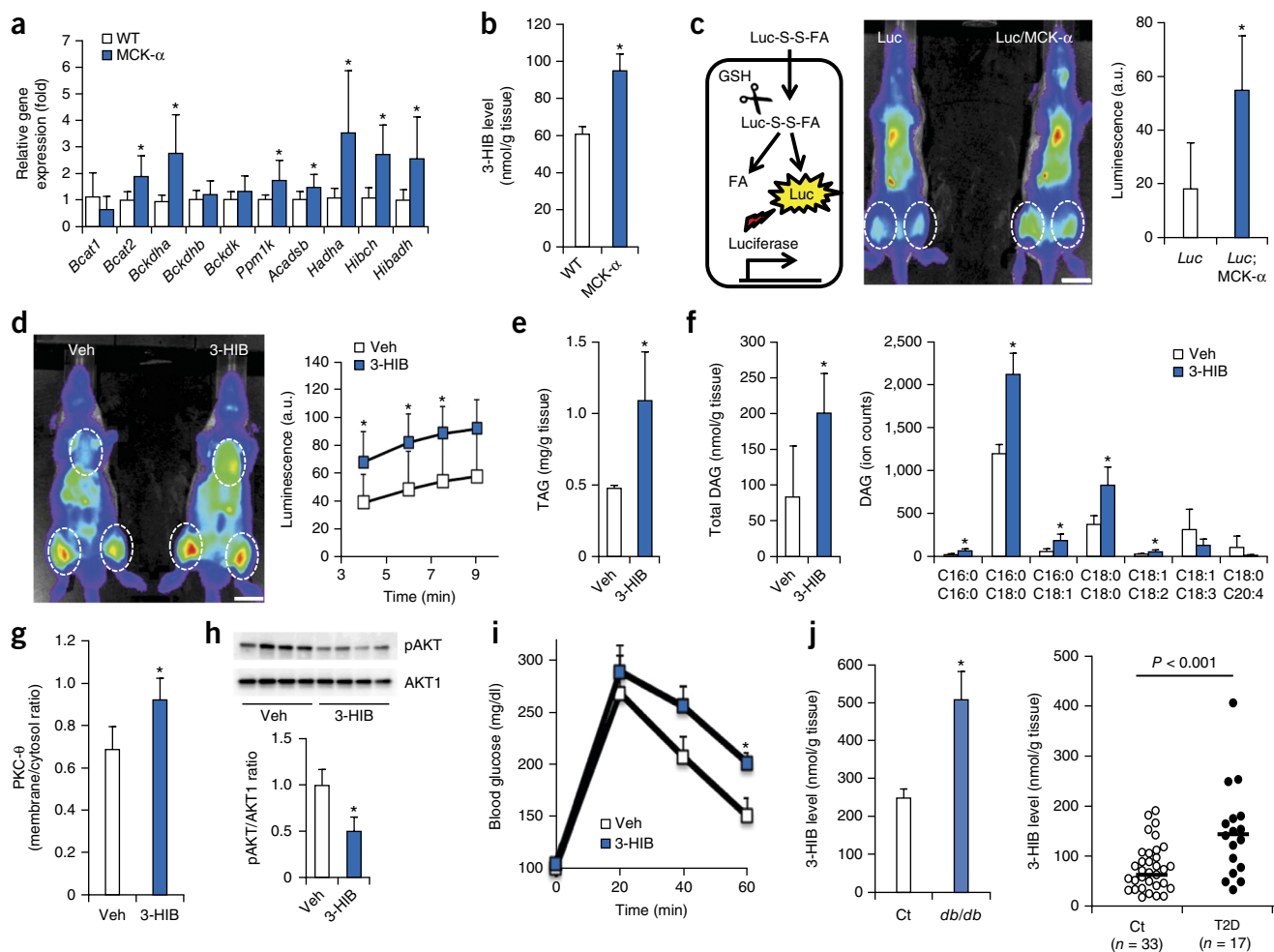


Figure 4 3-HIB induces fatty acid uptake *in vivo* and causes glucose intolerance. **(a,b)** qPCR analysis of valine metabolic enzyme expression (**a**; $n = 6$ per group) and measurement of 3-HIB levels (**b**; $n = 3$ per group) in muscle from wild-type (WT) or PGC-1 α -muscle specific transgenic mice (MCK- α). **(c)** Schematic of the fatty acid (FA) uptake assay *in vivo* (left). GSH, glutathione. Representative images (middle) and quantification (right, $n = 4$ per group) of fatty acid uptake in the thigh of luciferase transgenic (*Luc*) or *Luc*;MCK- α double-transgenic mice. Dashed circles indicate the heart and thigh regions used for quantification. Scale bar, 1 cm. **(d)** Representative images (left) and quantification (right, $n = 4$) of fatty acid uptake in the thigh of *Luc* mice fed with vehicle (Veh) or 3-HIB in a food paste for 1.5 h. Scale bar, 1 cm. **(e–i)** Measurements of triacylglyceride (**e**; $n = 3$ per group); total diglyceride (DAG; left in **f**; $n = 4$ per group) and specific DAG species (right in **f**; $n = 4$ per group); PKC- θ membrane translocation (**g**; $n = 4$ per group); levels of phosphorylated AKT (pAKT) and AKT1 as assessed by immunoblotting (**h**; $n = 4$ per group) in muscle; and systemic glucose tolerance (**i**; $n = 8$) of mice provided with vehicle (Veh) or 3-HIB in the drinking water for 2 weeks. **(j)** Measurements of 3-HIB levels in muscle of WT (Ct) and *db/db* mice (left; $n = 10$ per group) and in muscle biopsies of nondiabetic control (Ct) and people with type 2 diabetes (T2D) (right). Student's *t* test; * $P < 0.05$ versus control. In **j**, indicated *P* value was with Student's *t* test; with Mann-Whitney *U* test, $P < 0.005$ versus control. Data are mean \pm s.d. (**a,c–h**) or \pm s.e.m. (**b,i,j**).

lipid accumulation in mice that overexpress, or that are deficient in, PGC-1 α and PGC-1 β , as part of a broader comprehensive program controlled by these key metabolic transcription factors.

The provision of 3-HIB in the drinking water of wild-type (WT) mice led to a transient eightfold induction of 3-HIB in their serum and skeletal muscle, when compared to mice that did not receive this supplement (**Supplementary Fig. 9f–h**). Treated mice showed dramatically increased uptake of fatty acids into the heart and thigh, without any effect on vessel leakiness (**Fig. 4d** and **Supplementary Fig. 9i–k**), demonstrating that 3-HIB by itself is sufficient to induce fatty acid accumulation acutely *in vivo*. To test for a long-term effect, mice were provided with 3-HIB in their drinking water for 2 weeks, leading to a modest, 1.6-fold induction of 3-HIB levels in skeletal muscle (**Supplementary Fig. 10a**), similarly to that found in MCK- α mice (**Fig. 4b**) and in the skeletal muscle of diabetic mice (see *db/db* mice below). Mice that received 3-HIB showed accumulations

of triacylglycerides (TAG) and diglycerides (DAG) in their skeletal muscle (**Fig. 4e,f**), despite the absence of an increase in plasma fatty acid or TAG levels (**Supplementary Fig. 10b–e**) or apparent tissue damage (**Supplementary Fig. 10f**).

In accordance with the known inhibition of insulin signaling by DAG and by activated protein kinase C- θ (PKC- θ)⁴, 3-HIB administration to WT mice for 2 weeks led to an increase in the plasma membrane localization of PKC- θ in skeletal muscle (**Fig. 4g** and **Supplementary Fig. 10g**) and a decrease in the level of AKT1 phosphorylation, when compared to mice that did not receive 3-HIB supplementation (**Fig. 4h**). Treated mice showed systemic intolerance to a glucose load (**Fig. 4i**) and insulin resistance in hyperinsulinemic euglycemic clamp studies (**Supplementary Fig. 10h–j**). Neither hepatic gluconeogenesis gene expression nor glucose output was affected (**Supplementary Fig. 10k,l**), suggesting that 3-HIB has little effect on hepatic function. Taken together, these data demonstrate

that paracrine secretion of 3-HIB, an intermediate of BCAA catabolism, induces fatty acid uptake *in vivo*, and that 3-HIB causes excess accumulation of incompletely esterified lipids in skeletal muscle, blunted AKT signaling and glucose intolerance.

Valine is one of three BCAAs, all of which are essential dietary components. BCAAs are abundant in muscle, comprising up to 30% of muscle protein. The catabolic flux of BCAAs is tightly regulated in multiple organs, including skeletal muscle. Notably, all catabolic products of the three branched-chain α -keto acids are trapped inside the cell by covalent linkage to coenzyme A, with the single exception of 3-HIB (Fig. 3a). 3-HIB is thus ideally suited to act as a secreted reporter of BCAA catabolic flux in muscle. Excess BCAAs have recently been implicated in the progression to diabetes in mice, rats and humans^{1–3}. Data from the Framingham Heart Study, for example, show that an elevation in blood BCAA levels precedes the onset of diabetes by decades¹, but a mechanistic explanation for these observations has been lacking. Our data indicate that increased catabolic flux of BCAAs can cause the secretion of 3-HIB from muscle, leading to excess trans-endothelial fatty acid import into muscle, the accumulation of lipotoxic, incompletely esterified intermediates, such as DAG, and blunted insulin signaling. Consistent with this notion, we found significantly increased levels of 3-HIB in skeletal muscle from *db/db* mice and in muscle biopsies from people with diabetes (Fig. 4j). Findings of elevated 3-HIB levels in the serum of individuals with diabetes have also been previously reported^{15,16}. Notably, in muscle biopsies from both *db/db* mice and humans with diabetes, the elevation in 3-HIB levels occurred in the absence of any change in the gene expression of BCAA catabolic enzymes (Supplementary Fig. 10m,o). In contrast, the level of HIBADH protein—the enzyme that degrades 3-HIB—was decreased in muscle from *db/db* mice when compared to control mice without diabetes (Supplementary Fig. 10n), as has been reported in diabetic rats¹⁷. These findings suggest that post-transcriptional regulation may contribute to aberrant valine catabolism and insulin resistance. Individuals with severe 3-HIB aciduria and considerable neurological sequelae have also been described¹⁸, but the glucose homeostasis status of these individuals has not been reported.

In summary, our data highlight the importance of the vasculature in whole-body metabolic homeostasis, and they identify 3-HIB as a bioactive paracrine metabolite that regulates the trans-endothelial flux of fatty acids. These results uncover a cross-regulatory link between the catabolism of BCAAs and fatty acids, and provide a mechanistic explanation for how excess catabolic flux of BCAAs can lead to insulin resistance, a pathway that could potentially be targeted to treat diabetes.

METHODS

Methods and any associated references are available in the [online version of the paper](#).

Note: Any Supplementary Information and Source Data files are available in the [online version of the paper](#).

ACKNOWLEDGMENTS

Human endothelial colony forming cells (ECFCs) were kindly provided by J. Bischoff (Boston Children's Hospital). *Fatp4*^{-/-} and *Cd36*^{-/-} mice were kindly provided by J. Miner (Washington University School of Medicine) and J. Lawler (Harvard Medical School), respectively. *Flt1*^{fllox/fllox} and *Kdr*^{fllox/fllox} mice were kindly provided by Genentech. C.J. is supported by the Lotte Scholarship

and American Heart Association (AHA). S.F.O. is supported by the Crohn's and Colitis Foundation of America (Research Fellowship Award). S.W. is supported by the Toyobo Biotechnology Foundation. G.C.R. is supported by the US National Institute of Arthritis and Musculoskeletal and Skin Diseases (AR062128). J.R. is supported by the US National Institutes of Health (5 T32 GM7592-35). S.M.P. is supported by the US National Heart, Lung, and Blood Institute (NHLBI) (HL093234; HL125275) and the US National Institute of Diabetes and Digestive and Kidney Diseases (NIDDK) (DK095072). Q.C. and J.A.B. are supported by the NIDDK (DK098656; DK049210). Z.A. is supported by the NHLBI (HL094499), the AHA and the Geis Realty Group Emerging Initiatives Fund and Dean and Ann Geis.

AUTHOR CONTRIBUTIONS

C.J. led the studies and was directly involved in most experiments. S.F.O. assigned the structure of the paracrine factor as 3-HIB and performed mass spectrometric profiling. S.W., G.C.R., L.L., M.C.C., J.R., A.H., B.K., A.I., L.G.B., E.K. and A.J. assisted with experiments throughout, including qPCR, cell culture and animal studies. Q.C. and J.A.B. performed the mouse clamp studies. S.K. and A.M.W. performed the lipidomic studies. D.E.F. and S.H.L. isolated the human muscle biopsies. C.C.G. and S.M.P. performed the TEER studies. J.D.R. performed the metabolic flux analysis. D.L.K. and Z.A. oversaw the studies. C.J. and Z.A. designed experiments, interpreted results and wrote the paper. All authors discussed the results and commented on the manuscript.

COMPETING FINANCIAL INTERESTS

The authors declare no competing financial interests.

Reprints and permissions information is available online at <http://www.nature.com/reprints/index.html>.

- Wang, T.J. *et al.* Metabolite profiles and the risk of developing diabetes. *Nat. Med.* **17**, 448–453 (2011).
- Newgard, C.B. *et al.* A branched-chain amino acid-related metabolic signature that differentiates obese and lean humans and contributes to insulin resistance. *Cell Metab.* **9**, 311–326 (2009).
- Newgard, C.B. Interplay between lipids and branched-chain amino acids in development of insulin resistance. *Cell Metab.* **15**, 606–614 (2012).
- Shulman, G.I. Ectopic fat in insulin resistance, dyslipidemia, and cardiometabolic disease. *N. Engl. J. Med.* **371**, 1131–1141 (2014).
- Chan, M.C. & Arany, Z. The many roles of PGC-1 α in muscle—recent developments. *Metabolism* **63**, 441–451 (2014).
- Handschin, C. & Spiegelman, B.M. Peroxisome proliferator-activated receptor gamma coactivator 1 coactivators, energy homeostasis, and metabolism. *Endocr. Rev.* **27**, 728–735 (2006).
- Arany, Z. *et al.* HIF-independent regulation of VEGF and angiogenesis by the transcriptional coactivator PGC-1 α . *Nature* **451**, 1008–1012 (2008).
- Hagberg, C.E. *et al.* Vascular endothelial growth factor B controls endothelial fatty acid uptake. *Nature* **464**, 917–921 (2010).
- Roberts, L.D. *et al.* β -Aminoisobutyric acid induces browning of white fat and hepatic β -oxidation and is inversely correlated with cardiometabolic risk factors. *Cell Metab.* **19**, 96–108 (2014).
- Lin, J. *et al.* Transcriptional co-activator PGC-1 α drives the formation of slow-twitch muscle fibres. *Nature* **418**, 797–801 (2002).
- Arany, Z. *et al.* The transcriptional coactivator PGC-1 β drives the formation of oxidative type IIX fibers in skeletal muscle. *Cell Metab.* **5**, 35–46 (2007).
- Hatazawa, Y. *et al.* Metabolomic analysis of the skeletal muscle of mice overexpressing PGC-1 α . *PLoS One* **10**, e0129084 (2015).
- Henkin, A.H. *et al.* Real-time noninvasive imaging of fatty acid uptake *in vivo*. *ACS Chem. Biol.* **7**, 1884–1891 (2012).
- Choi, C.S. *et al.* Paradoxical effects of increased expression of PGC-1 α on muscle mitochondrial function and insulin-stimulated muscle glucose metabolism. *Proc. Natl. Acad. Sci. USA* **105**, 19926–19931 (2008).
- Avogaro, A. & Bier, D.M. Contribution of 3-hydroxyisobutyrate to the measurement of 3-hydroxybutyrate in human plasma: comparison of enzymatic and gas-liquid chromatography-mass spectrometry assays in normal and in diabetic subjects. *J. Lipid Res.* **30**, 1811–1817 (1989).
- Giesbertz, P. *et al.* Metabolite profiling in plasma and tissues of *ob/ob* and *db/db* mice identifies novel markers of obesity and type 2 diabetes. *Diabetologia* **58**, 2133–2143 (2015).
- Mullen, E. & Ohlendorf, K. Proteomic profiling of non-obese type 2 diabetic skeletal muscle. *Int. J. Mol. Med.* **25**, 445–458 (2010).
- Sasaki, M. *et al.* A severely brain-damaged case of 3-hydroxyisobutyric aciduria. *Brain Dev.* **23**, 243–245 (2001).

ONLINE METHODS

Fatty acid uptake assay. Confluent HUVECs (passage 2–8, Lonza #C2519AS) were transferred from a 10 cm dish to a gelatin-coated, 96-well, black, clear-bottom plate (Corning #3603), with empty corner wells for no-cell controls. After overnight incubation, the cells were serum-starved with endothelial basal medium (EBM2)-containing endothelial growth medium (EGM) supplements (Lonza #CC-3162) for at least 8 h. The cells were then treated with conditioned medium or 3-HIB (2.5 mM, Sigma #36105) for 1 h and briefly washed with phosphate-buffered saline (PBS). Then, Bodipy-FA (Molecular Probes #D3823), pre-incubated with fatty acid-free bovine serum albumin (BSA) (2:1 molar ratio) in PBS for 10 min in a 37 °C water bath, was added to the cells for 5 min at 37 °C. The solution of Bodipy-FA conjugated with BSA (Bodipy-FA/BSA) was then completely aspirated, and the cells were washed with 0.5% BSA in PBS for 1.5 min twice (50 μ l per well). To quench extracellular fluorescence, 0.4% trypan blue (MP Biomedicals #1691049) was added (50 μ l per well), and intracellular fluorescence was measured immediately (bottom-read) with a microplate reader (excitation 488 nm, emission 515 nm, cut-off 495 nm, SpectraMax M5, Molecular Probes). Readings from wells without Bodipy addition were used to subtract background signals. The cells were then quickly washed twice with PBS (50 μ l per well) and incubated with 44 μ M resazurin (#R7017, Sigma-Aldrich) in DMEM (50 μ l per well)-containing 10% fetal bovine serum (FBS) for 2 h. Resazurin fluorescence was then measured with a microplate reader (excitation 530 nm, emission 590 nm, cut-off 550 nm) and used to normalize Bodipy signals to cell number. Bodipy FL C16 (#D3821) and Bodipy FL C5 (#D3834) were purchased from Molecular Probes. Oleic acid-BSA was purchased from Sigma-Aldrich (#O3008). To block VEGF-B signaling in HUVECs, cells were pre-treated with 1 μ M SU11248 (sc-220178, Santa Cruz) for 10 min before conditioned-medium treatment, or conditioned medium was pre-incubated with 1 μ g per ml of sFLT1 (#14-923, Calbiochem) for 6 h at 4 °C with shaking, before being administered to endothelial cells. For trypsin treatment, conditioned medium was pre-incubated with 30 μ g per ml trypsin (Gibco) for 3 h at 37 °C, then incubated with 500 μ g per ml soy bean trypsin inhibitor (17075-029, Gibco) before being administered to endothelial cells.

Fatty acid transport assay. Isolation of primary rat brain endothelial cells was performed as described previously¹⁹. Cells were counted and seeded (5×10^4 cells per well) on a 0.4 μ m transwell (Corning #07-200-147), and they were then grown for 4 d until the cells formed compact monolayers. Meanwhile, C2C12 cells were differentiated into myotubes in a 24-well plate for 4 d. The brain endothelial cells in a transwell were then incubated with conditioned medium or 3-HIB (2.5 mM) for 1 h, and the transwell was inserted into the 24-well plate in which the C2C12 myotubes had been formed. Bodipy-FA/BSA or [U-¹³C]-palmitate/BSA in conditioned medium (80 μ l), with or without Dextran Texas-Red (70 kDa, Molecular Probes #D1830), was then added to the top chamber of the transwell. Conditioned medium containing only BSA (520 μ l) was added to the bottom chamber of the transwell. After each time point, 10 μ l of media was taken from the bottom chamber of the transwell to measure Bodipy-FA and Dextran Texas-Red fluorescence. To measure [U-¹³C]-palmitate metabolism in C2C12 myotubes, medium from the bottom chamber of the transwell was collected after 30 min of the transport assay and incubated with C2C12 myotubes for 1 h. Metabolites were then isolated from the C2C12 myotubes and quantified (UPenn Metabolomics Core, Princeton). Trans-endothelial electrical resistance (TEER) was measured as described previously²⁰.

Preparation of conditioned medium. C2C12 cells were grown in 10 cm dishes until 90% confluency and differentiated into myotubes with 5 μ g per ml insulin plus 5 μ g per ml transferrin (Sigma-Aldrich) in DMEM for 2 d, followed by 2% horse serum in DMEM (C2C12 differentiation media) for an additional 2 d. The cells were then infected with an adenovirus expressing GFP, PGC-1 α or PGC-1 β (ref. 21). Two days after infection, the cells were washed twice with PBS to remove adenovirus and incubated with 12 ml DMEM (with or without 2% horse serum) for 2 d. The effects of inhibitors on conditioned-medium activity were tested by addition of 2DG (5 mM), AKT VIII (5 μ M) or CHC (5 mM) with the DMEM. Conditioned medium was then collected, centrifuged

at 13,000g for 10 min at 4 °C, aliquoted and stored at –80 °C for future use. To generate PGC-1 α -expressing C2C12 cell lines, cells were infected either with retrovirus expressing human PGC-1 α or an empty-vector control²². Two days after infection, infected cells were selected with 2.5 μ g per ml puromycin for 2 d. To generate VEGF-B conditioned medium, a VEGF-B construct was obtained from the hORFeome Database #4833, cloned into the Gateway pcDNA-DEST40 vector (Invitrogen) and transfected into human embryonic kidney 293 T antigen (HEK293T) cells (ATCC). Fifteen hours after transfection, the cells were washed once with PBS and incubated with DMEM for 2 d before collection. Control conditioned medium was generated with a GFP plasmid construct (Addgene).

Cell culture. HUVECs (Lonza), primary rat brain endothelial cells and primary mouse heart and muscle endothelial cells were grown in EBM2-containing EGM supplements with 20% FBS. C2C12 and all other cell lines (ATCC) were grown in DMEM with 10% FBS. Isolation of primary myoblasts and endothelial cells was performed as described previously^{21,22}. Pericyte-like cells were differentiated from 10T1/2 cells with tumor growth factor (TGF)- β for 4 d, as described previously²³. For siRNA transfection, control siRNA (SIC001), *FATP3* siRNA (SASI_Hs01_00100092), *FATP4* siRNA (SASI_Hs01_00047530), *FLK1* siRNA (SASI_Hs01_00073461), *CD36* esiRNA (EHU089321), *HIBADH* siRNA (SASI_Hs01_00061462), *Hibch* siRNA (SASI_Mm02_00341755), *Hibadh* siRNA (SASI_Mm01_00120340) or *Vegfb* siRNA (SASI_Mm01_00114251, all from Sigma-Aldrich) were mixed with Lipofectamine RNAi Max (Invitrogen) in Opti-MEM (Sigma-Aldrich) for 20 min before being administered to cells.

Bodipy and immunofluorescence staining. Endothelial cells were grown on fibronectin-coated coverslips. The cells were washed once with PBS and fixed with 4% formaldehyde in PBS for 20 min at room temperature. The cells were then washed with washing buffer (0.1% Triton X-100 in PBS) three times for 30 min in total, incubated in blocking buffer (5% BSA in washing buffer) for 1 h and incubated with 1 μ g/ml Bodipy (Molecular Probes) in blocking buffer with or without a primary antibody (1:100 dilution) overnight at 4 °C. The cells were then washed with washing buffer three times for 30 min in total, and incubated with a secondary antibody (1:1,000 dilution in blocking buffer) for 3 h at room temperature. The cells were then washed with washing buffer six times for an hour in total, and mounted with DAPI mounting media (Molecular Probes #P36931). Images were then taken with a confocal microscope.

Quantitative RT-PCR (qPCR). mRNA was isolated using a TurboCapture mRNA kit (Qiagen) and reverse-transcribed with an RT kit (Applied Biosystems) according to the manufacturers' protocols. Primers used for qPCR are indicated in **Supplementary Table 1**.

Subcellular fractionation. All procedures were performed on ice. Fresh or frozen muscle (~150 mg) was minced with scissors and homogenized with a Dounce homogenizer (Corning, PYREX 2 ml, 30 strokes) in 1.3 ml homogenization buffer (0.1 M sucrose, 10 mM ethylenediaminetetraacetic acid, 46 mM KCl, 5 mM Na₃, 100 mM Tris-HCl pH 7.4 and protease inhibitors). The samples were then centrifuged at 4,000g for 10 min at 4 °C to precipitate nuclear fractions and cell debris. The supernatant (1 ml) was collected and mixed with 0.33 ml Opti-Prep (Sigma D1556, 60% iodixanol) to make a 15% iodixanol solution. Then, 1.33 ml of 40% iodixanol gradient solution, containing 0.1 M sucrose, 10 mM EDTA, 46 mM KCl, 5 mM Na₃, 10 mM Tris-HCl pH 7.4 and protease inhibitor, was added into a 4 ml ultracentrifuge tube, and the sample was carefully added on top of the gradient solution. Then, 1.33 ml of 5% iodixanol gradient solution, containing 0.1 M sucrose, 10 mM EDTA, 46 mM KCl, 5 mM Na₃, 10 mM Tris-HCl pH 7.4 and protease inhibitor, was carefully added on top of the sample. After ultracentrifugation at 80,000g for 16 h at 4 °C, fractions (250 μ l) were collected from the top. Each fraction was mixed with 6 \times sodium dodecyl sulfate (SDS) sample loading buffer, boiled for 5 min at 95 °C and loaded onto 4–20% gradient SDS-PAGE gels for immunoblotting.

Chromatography. Silica was baked to remove moisture and mixed with *n*-BuOH:MeOH (3:1, v/v) for packing. Conditioned medium was treated with

charcoal, lyophilized and resuspended in the same solvent. The column was eluted with three 5-ml additions of *n*-BuOH:MeOH (3:1), *n*-BuOH:MeOH (1:1) and 100% methanol. Each fraction was dried and resuspended in the EBM2 culture media for the Bodipy-FA uptake assay. For HILIC separation, active fractions were resuspended in-phase and injected into an HPLC (Dionex LC20 with GP50 quad pump and AD25 single wavelength UV detector) equipped with an HILIC column (Agilent HILIC plus, 4.6 mm × 100 mm × 3.5 μm). Ammonium acetate buffer (10 mM adjusted to pH 4.0) in a water/acetonitrile mix was used as eluent, initially at water:acetonitrile = 5:95 for 5 min, ramped to 55:45 over 8 min and held for 2 min. Fractions were collected every 30 s (for a total of 30 fractions).

Tandem mass spectrometry for structural identification. An HP-HILIC system (Waters BEH amide, 2.1 mm × 100 mm × 2.5 μm, equipped with HP1100 quad pump HPLC) coupled with tandem mass spectrometers (a Thermo Scientific LTQ XL instrument for structural identification and pathway analysis of 3-HIB, and a Thermo Scientific Q Exactive orbitrap instrument for high-sensitivity quantitation of *in vitro* and *in vivo* samples) was used. Ammonium formate buffer (2 mM adjusted at pH 9.0) in water/acetonitrile mix was used as eluent, initially at water:acetonitrile = 10:90 for 4 min, ramped to 40:60 over 3 min, held for 5 min for washing and re-equilibrated for the next run for 12 min. Selective ion monitoring (SIM)/parallel reaction monitoring (PRM) at 103.1 (hydroxybutyrate (HB) isomers), 106.1 (d3-2-HB standard) and 109.1 (d6-4-HB standard) were carried out for MS² spectra acquisition. Quantification of each HB species was carried out using the specific Q1→Q3 transition fingerprint (2-HB: 103→57, 3-HB:103→59, 3-HIB:103→73, 4-HB:103→85). ¹³C-2-valine was purchased from Sigma-Aldrich (#604917). ¹³C2-1,2-Leucine was purchased from Cambridge Isotope Laboratories (#CLM-3524). d3-2HB was purchased from CDN Isotopes (#D-7002) and d6-4HB was purchased from Cerilliant (#G-006).

Lipidomics. Liquid chromatography–mass spectrometry (LC-MS) grade acetonitrile (ACN), isopropanol (IPA), methanol and chloroform were purchased from Fisher Scientific. Diglyceride standard mix (d5-DAG, LM-6004) was purchased from Avanti Polar Lipids and leucine-enkephalin from Sigma-Aldrich. To extract lipids, vehicle or 3-HIB–fed mouse muscle samples were pulverized in liquid nitrogen, and lipids were extracted from muscle powder (50 mg) with a methanol-chloroform (2:1) mixture (300 μL), lysed by mechanical disruption (tissue laser from QIAGEN) with 25 pulses per sec for 2 min and sonicated for an additional 15 min. Chloroform and water were added (100 μl each), and the sample was vortexed. Organic and aqueous layers were separated by centrifugation for 7 min at 13,300 rpm at 4 °C. The d5-DAG internal standard mix was added to the organic layer, and samples were dried under N₂ gas. The dried lipid samples were re-dissolved in a mixture of 60% solvent A (40% H₂O, 60% ACN, 10 mM ammonium formate) and 40% solvent B (90% IPA, 10% ACN, 10 mM ammonium formate). The samples were centrifuged at 13,300 rpm for 5 min to remove fine particulates. The supernatant was transferred to a glass vial for ultra-performance liquid chromatography combined with a qTOF Xevo G2S (Waters) detector for high-throughput LC-MS lipidomics. For UPLC QTOF MS–based data acquisition for untargeted lipidomic profiling, each 10 μl sample was injected onto a reverse-phase column (XSELECTTM CSHTM C18, 2.1 mm × 100 mm × 2.5 μm) using an Aquity H-class UPLC system (Waters Corporation). Each sample was chromatographed for 9 min at a flow rate of 0.5 ml/min. The UPLC gradient consisted of 75% A and 25% B for 0.5 min, a quick ramp of 50% A and 50% B for 0.5 min, 25% A and 75% B for 4 min, followed by a ramp of 10% A and 90% B for 2 min, and finally a ramp to 1% A and 99% B for 2 min. The column eluent was introduced directly into the mass spectrometer. Mass spectrometry was performed with a positive ion–sensitive mode with a capillary voltage of 3,000 V and a sampling cone voltage of 40 °C. The desolvation gas flow was set to 800 l/h, and the temperature was set to 450 °C. The source temperature was set to 80 °C. Assessment of accurate mass was maintained by the introduction of a lock-spray interface of leucine-enkephalin (556.2771 *m/z*) at a concentration of 0.5 ng/μl in 50% aqueous acetonitrile and a rate of 5 μl/min. Data was acquired in the centroid MSe mode from 50–1,200 *m/z* mass ranges for both MS (low energy) and MSe (high energy) modes. Low-energy or fragmented

data were collected without collision energy, whereas high-energy or fragmented data were collected by using a collision-energy ramp from 15–40 eV. The entire set of triplicate sample injections was bracketed with a test mix of standard metabolites at the beginning and end of the run to evaluate instrument performance with respect to sensitivity and mass accuracy. The sample queue was randomized to remove bias. Lipid analysis and identifications were performed using Progenesis software (Waters Corporation). Fragmentation of endogenous DG (16:0/16:0)- *m/z* 551.50 Da, DG (16:0/18:0)-596.54 Da, DG (16:0/18:1)-577.51 Da, DG (18:0/18:0)-607.56 Da, DG (18:1/18:2)-601.51 Da, DG (18:1/18:3)-1234.07, and DG (18:0/20:4)-689.51 Da was confirmed by data-dependent acquisition and time-of-flight mass spectrometry (TOF-MS) methods, along with MSE.

Mouse models. All mouse experiments were performed according to procedures approved by the University of Pennsylvania or Beth Israel Deaconess Medical Center (BIDMC) Institutional Animal Care and Use Committees. MCK-α, MCK-β and muscle-specific PGC-1α and PGC-1β KO mice were described previously^{10,11,21}. For 3-HIB feeding, 12-week-old C57BL/6 male mice (Jackson Lab) were fed with 3-HIB (Sigma-Aldrich 36105) in drinking water (300 mg/kg/day) for 2 weeks. Free fatty acids (Cayman), TAG (Cayman) and DAG (Mybiosource) kits were used according to the manufacturers' protocols. For the glucose-tolerance test, 8-week-old male mice were fasted for 16 h and weighed, and a baseline blood glucose level was measured using a glucometer. Each mouse was intraperitoneally injected with sterilized 10% w/v D-glucose (10 μl/g body weight), and then blood glucose was measured at each time point. Hyperinsulinemic euglycemic clamp studies were performed as described previously²⁴. Luciferase-transgenic and *db/db* mice were purchased from Jackson Lab (#008450). Luciferin (Luc)-S-S-fatty acid was purchased from INTRACE MEDICAL SA. To measure fatty acid uptake *in vivo*, 10-week-old female luciferase-TG or luciferase/MCK-α double-transgenic mice were fasted for 16 h and then *ad lib* fed with food pasted mixed with 30 mM 3-HIB in water for 1.5 h. The mice were then anesthetized and intravenously injected with 100 μl of warm PBS containing 20 μM Luc-S-S-fatty acid and 10 μM fatty acid–free BSA. Luminescence was measured immediately after the injection of Luc-S-S-fatty acid using a Xenogen IVIS-50 bioluminescence-imaging system at the BIDMC Small Animal Imaging Core. Images and data quantification were performed by personnel blinded to treatment and genotype groups. To measure vessel leakiness *in vivo*, mice were anesthetized and intravenously injected with 50 μl of 2% Evans blue in PBS. After 5 min, blood was collected and intracardiac perfusion was performed with 100 ml PBS. Skeletal muscle was then isolated, minced with scissors in PBS, homogenized with metal beads and centrifuged at 13,000g for 10 min, and Evans blue in supernatants was quantified (absorbance at 611 nm) and normalized to total protein concentration, as measured by the BCA assay (Promega). To perform plasmid and siRNA electroporation into the tibialis anterior muscle, 8-week-old male mice were anesthetized with isoflurane, hair was removed from their legs and a small incision was made on the skin to expose the muscle. Then, 25 μg of CMV-EGFP plasmid (Addgene) with 5 μg of control or *Hibadh* siRNA in 25 μl sterilized saline was slowly injected into the muscle with an insulin syringe. The skin incision was then sutured, and electroporation was applied by touching the two pin electrodes around the injection site (voltage, 50 V/cm; pulse duration, 100 ms; frequency of pulses, 1 Hz). A train of total eight pulses (four pulses, then an additional four pulses after switching the position of the electrodes) was delivered. The left leg was injected with control siRNA, and the right leg was injected with *Hibadh* siRNA. After 9 d of recovery, the injected muscle was isolated, and GFP-positive muscle fibers (5–10 mg) were collected to measure TAG and protein concentrations.

Human samples. The cohort of skeletal muscle biopsy samples was described previously²⁵. Human studies were approved by the University of Pennsylvania institutional review board (IRB). Informed consent was obtained from all subjects.

Reagents. Anti-pan-actin (#4968), Anti-ERK1/2 (#9102), anti-pERK1/2 Thr 202/Tyr204 (#9101), anti-AKT (#4685), anti-pAKT Ser473 (#9271 all from Cell Signaling), anti-FATP3 (Proteintech 12943-1-AP), anti-FATP4 (Abnova

H00010999-M01), anti-PKC- θ (BD Transduction lab 610089), anti-Na,K ATPase A1 (Novus Biologicals NB300-146SS) and anti-HIBADH (Proteintech 13466-1-AP) antibodies were used for immunoblotting (1:1,000 dilution). Anti-occludin-1 (Abcam ab31721) and anti-calnexin (Thermo MA3-27) antibodies were used for immunostaining (1:200 dilution). Mitotracker Red CMXRos (Cell Signaling 9082S) was used for mitochondria staining. SSO (sc-208408) was purchased from Santa Cruz. Akt VIII (#124018) was purchased from Calbiochem. CHC (#5029) was purchased from Tocris. Recombinant VEGF-A (#293-VE-010) and VEGF-B (#767-VE-010) were purchased from R&D Systems. Human insulin (Humulin R U-100) was purchased from Harvard Drug Group (#821501). Membrane filters (MWCO 3 kDa #Z677094), Calcimycin (#C9275), 2,4-dinitrophenol (#D198501), 2-deoxyglucose (#D8375), activated charcoal (#C4386) and other chemicals were purchased from Sigma-Aldrich, unless otherwise stated.

Statistics. *P* values were calculated using the two-tailed Student's *t*-test. For statistical comparisons between study groups, two-way ANOVA was used, followed by Bonferroni *post hoc* testing. *P* < 0.05 was considered to be statistically significant. Data are displayed as mean \pm s.d. or standard error

(as indicated). All cell culture experiments included at least three biological replicates. All animal cohorts included at least three animals in each study group (as indicated). Animals were randomized to treatment groups.

19. Abbott, N.J., Hughes, C.C., Revest, P.A. & Greenwood, J. Development and characterisation of a rat brain capillary endothelial culture: towards an *in vitro* blood-brain barrier. *J. Cell Sci.* **103**, 23–37 (1992).
20. Xie, Z. *et al.* Vascular endothelial hyperpermeability induces the clinical symptoms of Clarkson disease (the systemic capillary leak syndrome). *Blood* **119**, 4321–4332 (2012).
21. Rowe, G.C. *et al.* Disconnecting mitochondrial content from respiratory chain capacity in PGC-1-deficient skeletal muscle. *Cell Reports* **3**, 1449–1456 (2013).
22. Sawada, N. *et al.* Endothelial PGC-1 α mediates vascular dysfunction in diabetes. *Cell Metab.* **19**, 246–258 (2014).
23. Darland, D.C. & D'Amore, P.A. TGF β is required for the formation of capillary-like structures in three-dimensional cocultures of 10T1/2 and endothelial cells. *Angiogenesis* **4**, 11–20 (2001).
24. Titchenell, P.M., Chu, Q., Monks, B.R. & Birnbaum, M.J. Hepatic insulin signalling is dispensable for suppression of glucose output by insulin *in vivo*. *Nat. Commun.* **6**, 7078 (2015).
25. Forman, D.E. *et al.* Analysis of skeletal muscle gene expression patterns and the impact of functional capacity in patients with systolic heart failure. *J. Card. Fail.* **20**, 422–430 (2014).